© 2014. Published by The Company of Biologists Ltd | Journal of Cell Science (2014) 127, 1899–1910 doi:10.1242/jcs.137422

RESEARCH ARTICLE

Consequences of the disease-related L78R mutation for dimerization and activity of STAT3

Tamás Domoszlai, Antons Martincuks, Dirk Fahrenkamp, Hildegard Schmitz-Van de Leur, Andrea Küster and Gerhard Müller-Newen*

ABSTRACT

Signal transducer and activator of transcription 3 (STAT3) is a transcription factor that is centrally involved in diverse processes including haematopoiesis, immunity and cancer progression. In response to cytokine stimulation, STAT3 is activated through phosphorylation of a single tyrosine residue. The phosphorylated STAT3 dimers are stabilized by intermolecular interactions between SH2 domains and phosphotyrosine. These activated dimers accumulate in the nucleus and bind to specific DNA sequences, resulting in target gene expression. We analysed and compared the structural organizations of the unphosphorylated latent and phosphorylated activated STAT3 dimers using Förster resonance energy transfer (FRET) in fixed and living cells. The latent dimers are stabilized by homotypic interactions between the N-terminal domains. A somatic mutation (L78R) found in inflammatory hepatocellular adenoma (IHCA), which is located in the N-terminal domain of STAT3 disturbs latent dimer formation. Applying intramolecular FRET, we verify a functional role of the SH2 domain in latent dimer formation suggesting that the protomers in the latent STAT3 dimer are in a parallel orientation, similar to activated STAT3 dimers but different from the antiparallel orientation of the latent dimers of STAT1 and STAT5. Our findings reveal unique structural characteristics of STAT3 within the STAT family and contribute to the understanding of the L78R mutation found in IHCA.

KEY WORDS: JAK-STAT signalling, STAT3, Dimerization, Inflammatory hepatocellular adenoma, Hyper-IgE syndrome, Fluorescence microscopy, FRET

INTRODUCTION

The signal transducers and activators of transcription (STATs) are dual function proteins which receive an activating signal from the cell surface and carry it toward the nucleus to induce gene transcription (Stark and Darnell, 2012). The STAT protein family consists of seven members (STAT1, STAT2, STAT3, STAT4, STAT5a, STAT5b and STAT6) that share a common structural organization represented by six distinct and functionally conserved domains: N-terminal domain (NTD), coiled-coil domain (CCD), DNA-binding domain (DBD), linker domain (LD), Src homology 2 domain (SH2) and the C-terminally located transactivation domain (TAD) (Fig. 1A). Numerous ligands are able to activate STAT transcription factors, including cytokines, growth factors and hormones, as well as oncogenic proteins such as mutated tyrosine kinases (Aggarwal et al., 2009). The dysregulated activation of STAT signalling is involved in chronic inflammation (O'Sullivan et al., 2007) and cancer, including blood malignancies and solid tumours (Yu and Jove, 2004).

In the canonical view of JAK-STAT signalling, cytokines are recognized by cell surface receptors that are associated with Janus tyrosine kinases (JAKs). Upon ligand binding the JAKs become activated and phosphorylate tyrosine residues of the receptor. These phosphotyrosine motifs act as docking sites for proteins containing Src homology 2 (SH2) domains, including various adaptor proteins, negative regulators, such as suppressor of cytokine signalling (SOCS) proteins and phosphotyrosine phosphatases (e.g. SHP2), or, most importantly, transcription factors of the STAT family. STATs are recruited to the receptor and are phosphorylated on a single tyrosine residue by JAKs. The phosphorylated STATs form homo- or hetero-dimers through reciprocal interactions between the phosphotyrosine motif of one and the SH2 domain of the other protomer. The dimerized STAT molecules translocate to the nucleus, bind to specific response elements and activate target gene expression (Levy and Darnell, 2002).

In recent years, several publications have reported on preformed (latent, unphosphorylated) STAT dimers (Haan et al., 2000; Kretzschmar et al., 2004; Schröder et al., 2004), STAT tetramers at specific gene promoters (Zhang and Darnell, 2001), but also on conglomerates of higher molecular masses such as statosomes (Ndubuisi et al., 1999), nuclear bodies (Herrmann et al., 2004) or paracrystals (Droescher et al., 2011). Moreover, biological functions of STATs independent of tyrosine phosphorylation have been described. These non-canonical functions have been demonstrated to be involved in controlling heterochromatin and microtubule stability or regulating metabolic functions in mitochondria (Mohr et al., 2012).

STAT3 has been identified as a key player in chronic inflammation, autoimmune diseases and tumorigenesis. In contrast to the cytokine-induced transient activation, STAT3 is persistently activated in a variety of human cancers, mostly as a consequence of deregulated upstream signalling pathways (Yu and Jove, 2004). More recently, mutations targeting structural domains of STAT3 have been associated with some diseases, such as hyper-IgE syndrome (HIES) (Holland et al., 2007), large granular lymphocytic leukaemia (LGL leukaemia) (Koskela et al., 2012) or inflammatory hepatocellular adenoma (IHCA) (Pilati et al., 2011).

Here, we used Förster resonance energy transfer (FRET) to study the dimers of STAT3 before and after activation, to

Institut für Biochemie und Molekularbiologie, RWTH Aachen University, 52074 Aachen, Germany.

*Author for correspondence (mueller-newen@rwth-aachen.de)

Received 25 June 2013; Accepted 31 January 2014

Journal of Cell Science (2014) 127, 1899–1910 doi:10.1242/jcs.137422

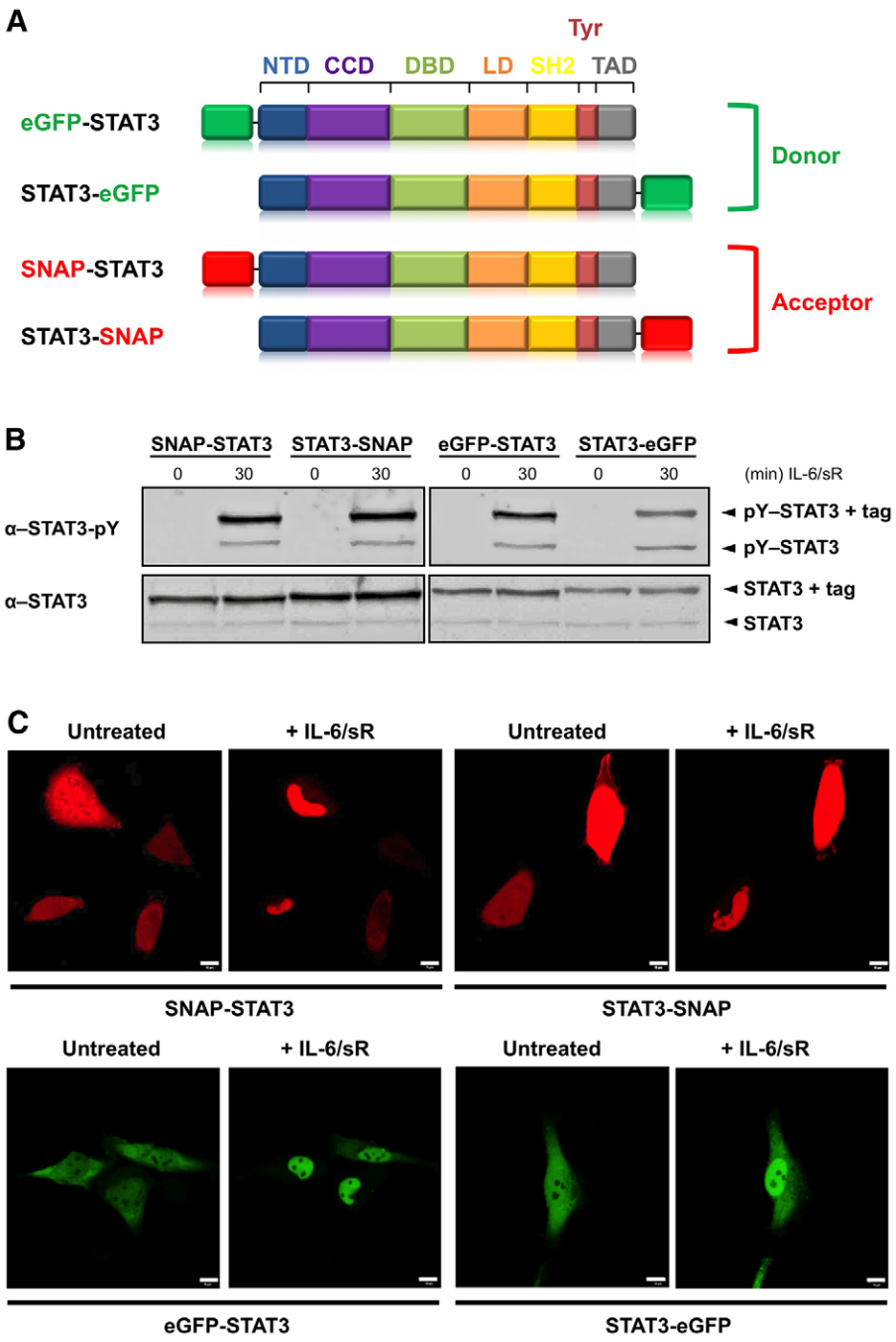

Fig. 1. Characterization of STAT3 fusion protein constructs. (A) Representation of differently labelled STAT3 constructs used in FRET experiments. eGFP-tagged STAT3 proteins serve as FRET donors, SNAP-tagged proteins labelled with TMRstar substrate are FRET acceptors. NTD, N-terminal domain; CCD, coiled-coil domain; DBD, DNA-binding domain; LD, linker domain; SH2, SH2 domain; Tyr, tyrosine motif; TAD, transactivation domain. (B) Functional analysis of tagged STAT3 constructs. HeLa cells were transfected with the indicated expression vectors encoding SNAP–STAT3, STAT3–SNAP, eGFP–STAT3 or STAT3–eGFP. Cells were stimulated with 20 ng/ml IL-6 and 500 ng/ml soluble IL-6 receptor (sR) for 30 minutes or left unstimulated. Lysates were analysed by immunoblotting using antibodies against STAT3 phosphotyrosine 705 (pY-STAT3) and STAT3. (C) Ligand induced nuclear accumulation of STAT3 fusion proteins. Localization of SNAP–STAT3 and STAT3–SNAP labelled with TMRstar (upper panel) and eGFP–STAT3 and STAT3–eGFP (lower panel) analysed in living cells after stimulation for 30 minutes with 20 ng/ml IL-6 and 500 ng/ml soluble IL-6 receptor using confocal microscopy in living HeLa cells. Scale bars: 10 μm.

determine the orientations of the protomers in these dimers and to analyse the structural and functional consequences of the somatic L78R mutation found in IHCA.

RESULTS

Characterization of STAT3 fusion protein constructs

To investigate the homodimerization of STAT3 with FRET imaging we used eGFP (enhanced green fluorescent protein) as a donor fluorophore and TMRstar coupled to the SNAP tag as an acceptor fluorophore. The target protein was labelled N- or C-terminally with the donor or with the acceptor fluorophore resulting in four different fusion protein constructs (Fig. 1A).

To study the expression and functional properties of the STAT3 fusion constructs, HeLa cells were transfected with plasmids encoding SNAP–STAT3, STAT3–SNAP, eGFP–STAT3 or STAT3–eGFP. Cells were stimulated with IL-6 and soluble IL-6 receptor for 30 minutes or left untreated and lysates were analysed by immunoblotting (Fig. 1B). After cytokine stimulation, all constructs were phosphorylated at tyrosine residue 705, demonstrating that labelling with eGFP or SNAP tag (N- or C-terminally) does not interfere with the phosphorylation of the fusion protein, in good agreement with previously published data from our laboratory (Herrmann et al., 2004) and from others (Huang et al., 2007). For further functional analysis, the tagged STAT3 proteins were expressed in HeLa cells and the nuclear translocation in response to IL-6 and soluble IL-6 receptor stimulation was monitored in real time with confocal microscopy (Fig. 1C). All four constructs accumulated

Journal of Cell Science (2014) 127, 1899–1910 doi:10.1242/jcs.137422

in the nucleus in response to cytokine treatment verifying the fusion constructs as functional molecules for further experiments.

Acceptor photobleaching FRET

To study the interactions and conformational changes between two fluorescently labelled STAT3 molecules, we measured FRET with the acceptor photobleaching technique (Fig. 2A). Briefly, when a suitable donor and acceptor fluorophore are in close proximity, non radiative energy transfer (FRET) can occur between the molecules. Disruption of the energy transfer by selective bleaching of acceptor molecules (TMRstar) leads to an increase in donor (eGFP) fluorescence due to loss of quenching. To set up the experimental conditions for FRET detection, background and maximal FRET signal were analysed with appropriate negative and positive FRET controls.

As a negative control, eGFP was coexpressed with TMRstar–STAT3 resulting in a very low FRET signal (2.28%±1.01, mean±s.d.) (Fig. 2A, lower panel; Fig. 2B). Additional controls including mitochondrial cytochrome oxidase 8-2 subunit (Cox8A)–TMRstar coexpressed with eGFP or donor (eGFP) and acceptor (TMRstar–STAT3) expressed alone also showed low FRET efficiencies of 1.05%±0.66, 0.69%±1.12 and 0.60%±0.98 respectively (data not shown). Energy transfer efficiencies of TMRstar-loaded SNAP tag fused with an eight-amino-acid linker to eGFP served as a positive control. A FRET efficiency of 17.55%±4.84 was measured, representing the highest detectable energy transfer signal in our setup (Fig. 2A, upper panel; Fig. 2B).

In further experiments, the selection of cells for FRET measurements and microscope settings were based on the positive control (donor and acceptor fluorophores are equimolar), to avoid the influence of different donor-to-acceptor ratios, which beside other parameters (spectral overlap, molecular distance, applied method) have been shown to affect FRET efficiency (Berney and Danuser, 2003).

Conformation of STAT3 dimers prior to and after activation

It has been well established and demonstrated by various techniques that STATs are able to form stable dimers prior to stimulation (Braunstein et al., 2003; Haan et al., 2000; Kretzschmar et al., 2004; Schröder et al., 2004; Stancato et al., 1996). Our previous findings have shown the essential role of the NTD in the formation of unphosphorylated STAT3 dimers (Vogt et al., 2011), similar to other STAT family members (Wenta et al., 2008). However, the conformation and orientation of the protomers in the preformed dimer are still unknown. In our model (Fig. 3A), we propose two possible conformations of unphosphorylated STAT3

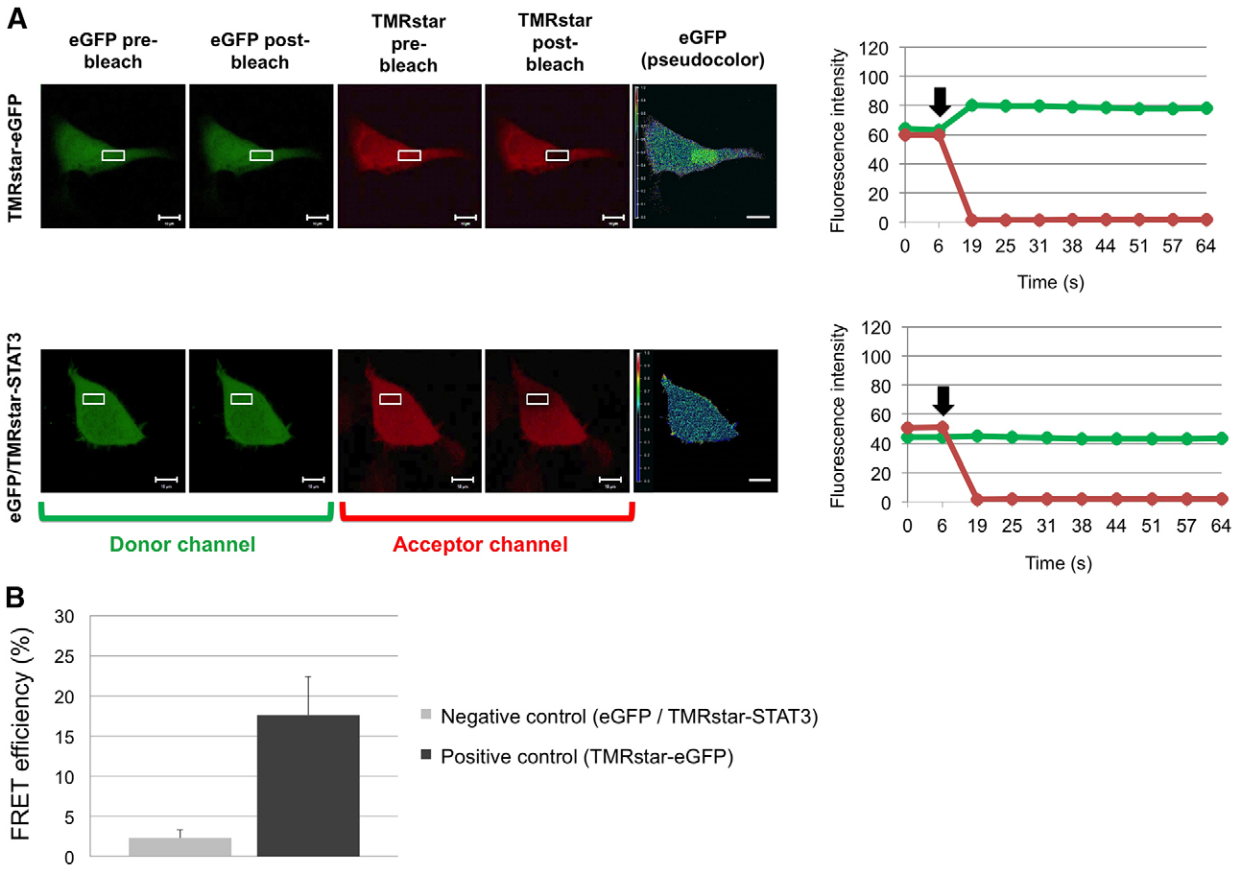

Fig. 2. Acceptor photobleaching FRET. (A) As positive FRET control, a TMRstar-labelled SNAP–eGFP fusion construct (TMRstar–eGFP) showed a specific increase in eGFP (donor) fluorescence after acceptor (TMRstar) bleaching (indicated by the arrow) in a rectangular region of interest, as it is visualized in a pseudocolour image of eGFP intensity. In the negative control, where eGFP was coexpressed with TMRstar–STAT3, no intensity changes in eGFP signal was visible after bleaching of TMRstar. Scale bars: 10 μm. (B) Representative FRET control experiments. eGFP alone, as donor fluorophore coexpressed with TMRstar–STAT3 construct served as negative control in FRET measurements (FRET efficiency: 2.28%±1.01). The positive control consisted of the TMRstar–eGFP fusion construct, where the SNAP tag was labelled with TMRstar substrate as acceptor fluorophore (FRET efficiency 17.55%±4.84) (mean±s.d., n=20 cells).

Journal of Cell Science

Journal of Cell Science (2014) 127, 1899–1910 doi:10.1242/jcs.137422

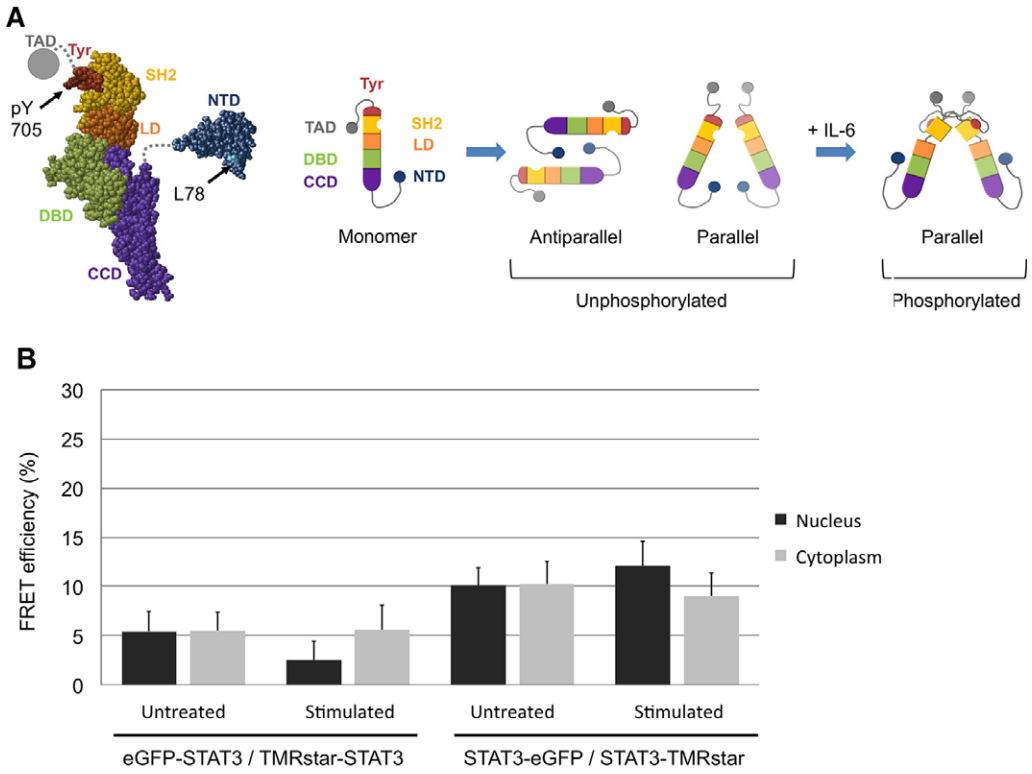

Fig. 3. In latent and activated STAT3 dimers, the protomers are aligned in parallel. (A) Possible STAT3 dimer formations. The structure of STAT3 is shown in spacefill mode based on Becker et al. (Becker et al., 1998), PDB ID 1BG1. The structure of the NTD is taken from STAT4 (Vinkemeier et al., 1998), PDB ID 1BGF. Structural information on the TAD does not exist. Amino acids important for this study are marked with arrows. In the schemes, the colour code for the individual domains is maintained as in Fig. 1A. Schemes are designed in analogy to those used by Mertens et al. (Mertens et al., 2006). STAT3 monomers prior to stimulation dimerize in a parallel or antiparallel orientation. In both conformations the NTDs are localized close to each other. Following cytokine addition (+ IL-6), STAT3 molecules get phosphorylated and dimerize in a parallel form (stabilized by reciprocal interactions between phosphotyrosine residues and SH2 domains) where the NTDs are widely separated from each other. Only in the parallel dimer are the C-termini close to each other. (B) FRET efficiencies (%) between N- and C-terminally labelled STAT3 molecules. Dimerization of STAT3 was followed by the analysis of FRET signals between N- and C-terminally labelled STAT3 monomers (carrying donor and acceptor fluorophore at the N- or C-terminus of the host molecule) in the nuclear and cytoplasmic regions of fixed HeLa cells, before and after addition of IL-6 (mean±s.d., n=36–40 cells).

dimers: (1) antiparallel, with the two C-terminal regions localized at the opposite ends of the dimer, similar to the conformations found for latent STAT1 (Mertens et al., 2006) and latent STAT5a (Neculai et al., 2005); and (2) parallel, with the C-termini of the protomers located at the same end of the dimer, similar to the activated STAT3 dimer (Becker et al., 1998).

To follow the orientation of the NTDs during dimerization, eGFP–STAT3 and TMRstar–STAT3 (carrying the donor and acceptor fluorophore at the N-terminus of the host molecule) were coexpressed and examined with acceptor photobleaching FRET in fixed HeLa cells (Fig. 3B). Prior to activation, a significant FRET signal ($P<0.001$) was detectable between the NTDs compared with the negative control in both compartments (nucleus, 5.42%±2.05; cytoplasm, 5.50%±1.91; mean±s.d.), indicating the existence of latent STAT3 dimers and the close proximity of NTDs in this structure.

Upon activation STAT3 molecules get phosphorylated, translocate to the nucleus and act as transcription factors through binding to specific DNA sequences. This activated nuclear STAT3 fraction has completely lost the FRET signal, indicating that the NTDs have moved away from each other to form the activated STAT3 dimer. FRET efficiencies in the cytoplasm were not significantly different ($P=0.829$) from untreated cells, indicating the dominance of a non-activated or de-activated STAT3 dimer fraction in this compartment after 30 minutes of cytokine stimulation. These findings are in good agreement with data generated with STAT5a, where stimulation also resulted in a loss of FRET between the NTDs of CFP–STAT5a and YFP–STAT5a (Neculai et al., 2005).

With C-terminally labelled STAT3 (STAT3–eGFP and STAT3–TMRstar) strong FRET signals were detected prior to activation in both cytoplasm and nucleus (Fig. 3B) indicating the close proximity of the C-terminal domains in the preformed dimer (nucleus, 10.09%±1.79; cytoplasm, 10.26%±2.26). FRET analysis revealed an increased energy transfer efficiency only in the nuclear compartment after cytokine treatment, in comparison with untreated cells ($P=0.00016$), which is in good agreement with the previously published FRET results on STAT3–CFP and STAT3–YFP constructs (Cimica et al., 2011; Kretzschmar et al., 2004). However, this difference compared to non-stimulated sample is not that high to support an antiparallel orientation, but rather a parallel orientation of the protomers in the activated STAT3 dimer. In support of this hypothesis, measurements on C-terminally truncated STAT3 (ΔTAD-STAT3–TMRstar) and STAT3–eGFP, showed no detectable changes in FRET efficiency after stimulation (data not shown). Similar FRET experiments performed with living HeLa cells gave essentially the same results showing that fixation of cells does not affect FRET efficiencies (data not shown).

Journal of Cell Science (2014) 127, 1899–1910 doi:10.1242/jcs.137422

Homotypic interactions between NTDs of STAT3

To further define the interdomain interactions during dimer formation of latent STAT3, we generated a construct which encodes the NTD of STAT3 and analysed the capability of the isolated NTD to interact with full-length STAT3. In HeLa cells transfected with constructs encoding TMRstar–NTD and eGFP–STAT3 or STAT3–eGFP (Fig. 4A) a strong FRET signal was detectable (nucleus, 9.34%±3.62; cytoplasm, 8.72%±2.94; mean±s.d.) when the donor fluorophore was localized at the N-terminus of the full-length protein. In contrast, transfection of STAT3–eGFP and TMRstar–NTD resulted in low FRET signals (nucleus, 2.64%±2.23; cytoplasm, 2.76%±1.94) indicating that the interaction is localized at the N-terminal region of STAT3. Measurements on N-terminally deleted STAT3 (STAT3-ΔNTD–eGFP), revealed no significant FRET between the two constructs (nucleus, 1.76±1.25%; cytoplasm, 1.45±1.57%), indicating that no other STAT3 domains are involved in the N-terminal interactions. This is in good agreement with GST pulldown assays from cellular lysates, where also no interaction between the N-terminal fragment and other structural domains of STAT3 was detectable (Zhang et al., 2002). Our data demonstrate the capability of the TMRstar–NTD construct to interact with full-length STAT3 and verify the NTD as one interaction surface, similar to previous publications, showing the capability of NTDs of other STATs to dimerize with themselves (Ota et al., 2004).

The somatic mutation L78R of STAT3, found in IHCA, disrupts the homotypic interaction between the NTDs

Next, we wanted to know whether a somatic mutation in the NTD of STAT3 found in human IHCA interferes with the NTD–NTD interaction. For this purpose the point mutant L78R was generated in analogy to the somatic mutation (Pilati et al., 2011) (Fig. 4B). As in case of the wild-type construct we fused a SNAP tag to the mutated NTD and tested the interaction with full-length STAT3 using FRET analysis (Fig. 4C). The single mutation in the N-terminal fragment resulted in the complete loss of FRET between the NTDs of STAT3 (nucleus, 1.62%±1.37; cytoplasm, 1.37%±1.31, mean±s.d.; Fig. 4C) in comparison to wild-type (Fig. 4A). Involvement of the L78 residue in the dimerization of NTDs of STAT3 suggests a dimer interface similar to STAT1 where the NTDs carrying a L78 mutation were properly folded but monomeric (Chen et al., 2003).

To analyse to what extent the isolated NTD interferes with STAT3 dimerization, HeLa cells were transfected with SNAP–NTD and STAT3–YFP. Cellular lysates were analysed by blue-native PAGE and the fluorescence of STAT3–YFP was detected with a fluorescence scanner (Fig. 4D). In cells expressing STAT3–YFP alone, STAT3 monomers and preformed dimers were detected, as has been shown previously (Vogt et al., 2011). Upon overexpression of SNAP–NTD, the dimers disappear in a dose-dependent manner. NTD-mediated interactions are of functional importance on promoters, such as the α2-macroglobulin gene promoter, that require tetramerization of activated STATs at adjacent interferon-γ-activated sequence (GAS) sites (Zhang and Darnell, 2001). Indeed, overexpression of the STAT3 NTD inhibits α2-macroglobulin gene induction in HepG2 cells in response to IL-6, as shown by a reporter gene assay (Fig. 4E, left panel). The NTD harbouring the L78R mutation does not interfere with gene induction. Thus, the interfaces of the STAT3 NTD involved in latent dimer formation and tetramerization on promoters seem to be very similar. Moreover, disturbing NTD interactions by a selective inhibitor can interfere with STAT3 activity on a subset of promoters that respond to unphosphorylated STAT3 (Timofeeva et al., 2013).

Characterization of the STAT3 L78R mutant

To elaborate these findings, two STAT3 constructs were generated carrying the specific point mutation at leucine L78 in full-length STAT3: SNAP–STAT3(L78R) and STAT3(L78R)–SNAP (Fig. 5A). To analyse the capability of L78R mutated STAT3 to form dimers prior to cytokine addition, FRET was measured, in a similar procedure to the wild-type measurements, on two different FRET pair combinations: eGFP–STAT3 and TMRstar–STAT3(L78R), and STAT3–eGFP and STAT3(L78R)–TMRstar (Fig. 5B). In all cases, no significant FRET signal was detectable prior to stimulation clearly indicating that the L78R mutated STAT3 molecules cannot form dimers in the latent state, similar to the N-terminally truncated STAT3 construct (Vogt et al., 2011). With the C-terminally labelled constructs, FRET was detectable after cytokine addition (nucleus, 6.61%±1.82; cytoplasm, 6.70%±1.93, mean±s.d.) demonstrating that the L78R mutation does not prevent the formation of activated STAT3 dimers. As in case of wild-type STAT3, the *in vitro* findings on fixed cells were repeated and confirmed in experiments with living cells (data not shown). In summary, our findings verify the importance of NTD interactions in stabilizing the preformed STAT3 dimer and highlight the relevance of the L78 residue in the dimer interface.

Upon transfection of HeLa cells, SNAP–STAT3(L78R) and STAT3(L78R)–SNAP were expressed and phosphorylated on Tyr705 after cytokine addition to a comparable extent, indicating that localization of the tag does not interfere with phosphorylation (Fig. 5C). However, although overexpressed, hardly any phosphorylation of STAT3(L78R) could be detected in the absence of a stimulus.

To characterize STAT3(L78R) in more detail, $MEF^{\Delta/\Delta}$ cells lacking endogenous STAT3 were stably transfected with fluorescent STAT3(L78R)–CFP–YFP [STAT3(L78R)-CY] and compared with established and well-characterized $MEF^{\Delta/\Delta}$ cells expressing wild-type STAT3–CFP–YFP (STAT3-CY) (Vogt et al., 2011) in a live-cell imaging experiment (Fig. 5D). Compared to the preferentially cytoplasmic localization of STAT3-CY wild-type, the L78R mutant is more equally distributed between the cytoplasm and nucleus (Fig. 5D, upper images), similar to the distribution of STAT3 lacking the NTD (Vogt et al., 2011). Upon stimulation, both proteins enter the nucleus with similar kinetics (Fig. 5D, middle panel). Upon removal of the stimulus both proteins redistribute to the initial state after about 3 h (Fig. 5D, lower panel, best seen for cells marked with arrows). Thus, the L78R mutant does not show any gross changes in nuclear accumulation and redistribution.

The stably transfected $MEF^{\Delta/\Delta}$ cells were also used to analyse tyrosine phosphorylation of STAT3(L78R)-CY in comparison with STAT3-CY wild-type (Fig. 5E). Impairment of latent dimer formation in the STAT3(L78R) mutant does not have any influence on the sensitivity of the protein upon stimulation of IL-6 neither at low doses of the cytokine (Fig. 5E, upper panel) nor at early time points (Fig. 5E, middle panel). However, upon pulse stimulation with IL-6, phosphorylation of STAT3(L78R) is prolonged compared to wild-type (Fig. 5E, lower panel). Again, no phosphorylation of the L78R mutant is detectable in the absence of a stimulus.

Importance of the SH2 domain in latent dimerization of STAT3

It has been shown that the interaction of the isolated NTDs of STAT3 is of low affinity (millimolar range) compared to other

Journal of Cell Science (2014) 127, 1899–1910 doi:10.1242/jcs.137422

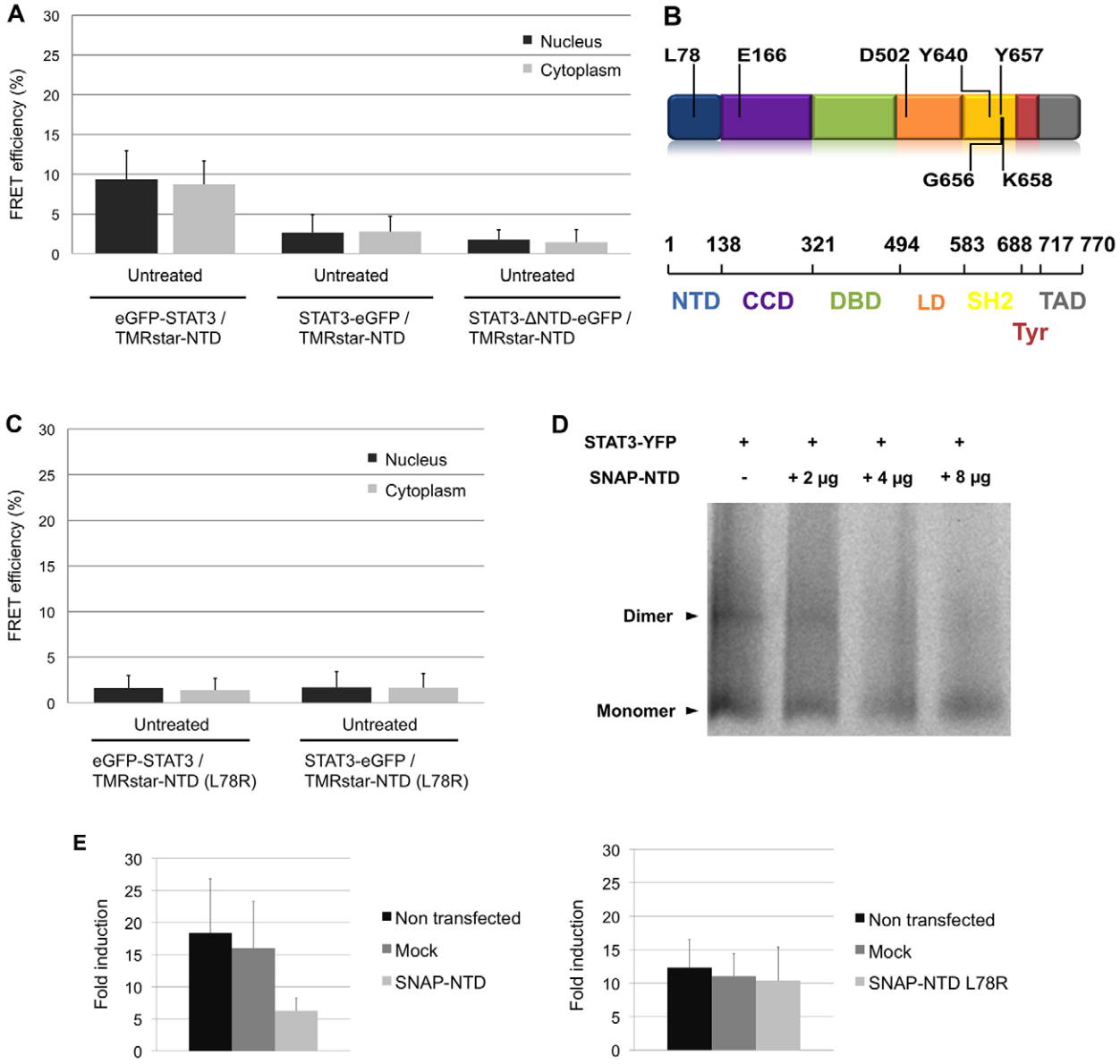

Fig. 4. The L78R somatic mutation disrupts the homotypic interaction between the NTDs of STAT3. (A) Homotypic N-terminal domain interactions. FRET efficiencies (%) of TMRstar–NTD with different STAT3–eGFP constructs. FRET results demonstrate the capability of the isolated N-terminal domain to interact with STAT3 through homotypic interactions between the N-terminal domains (mean±s.d., n=30 cells). (B) Distribution of STAT3 somatic mutations identified in IHCAs. The amino acid changes affect the N-terminal, coiled-coil, linker and the SH2 domain of the molecule, resulting in a mutant STAT3, which has been described to exhibit constitutive activity. (C) L78R mutated N-terminal domain does not interact with STAT3. A single amino acid mutation in the N-terminal domain leads to the NTD–NTD interdomain interaction being abolished. The detectable FRET efficiencies in both cases are indistinguishable from the background, eGFP–STAT3 and TMRstar–NTD(L78R) (nucleus, 1.62%±1.37; cytoplasm, 1.37%±1.31) and STAT3–eGFP and TMRstar-NTD(L78R) (nucleus, 1.70%±1.74; cytoplasm, 1.65%±1.56). (mean±s.d., n=30 cells). (D) Overexpression of the NTD interferes with the formation of latent STAT3 dimers. HeLa cells were transfected with expression vectors encoding STAT3–YFP and SNAP–NTD as indicated. At 24 h after transfection, cellular lysates were analysed by blue-native PAGE. STAT3–YFP was detected with a fluorescence scanner. (E) SNAP–NTD but not SNAP–NTD(L78R) interferes with the STAT3-mediated induction of the α2-macroglobulin gene. HepG2 cells were transfected with an expression vector encoding SNAP–NTD or SNAP–NTD(L78R) as indicated. Non-transfected and mock-transfected cells served as controls. Cells were stimulated with IL-6 (20 ng/ml) for 4 h and activity of the α2-macroglobulin promoter was measured with a reporter gene assay. Results are mean±s.d.

members of the STAT family (micromolar range) (Wenta et al., 2008) suggesting that additional interfaces are involved in the latent STAT3 dimer. FRET studies on SH2-mutated STAT3 (R609Q) revealed the need of an intact SH2 domain for preformed dimerization (Kretzschmar et al., 2004). This specific mutation has a strong influence on the overall functionality of STAT3 and leads to a non functional SH2 domain (Hemmann et al., 1996) preventing receptor recruitment and phosphorylation of STAT3 (Herrmann et al., 2007).

We applied intramolecular FRET (donor and acceptor fluorophores localized at the same host molecule; Fig. 6A) to analyse the effect of the R609Q mutation on the overall STAT3 structure. Double tagged wild-type STAT3 (Fig. 6B) prior (nucleus, 6.68%±1.24; cytoplasm, 6.48%±1.39; mean±s.d.) or

Journal of Cell Science (2014) 127, 1899–1910 doi:10.1242/jcs.137422

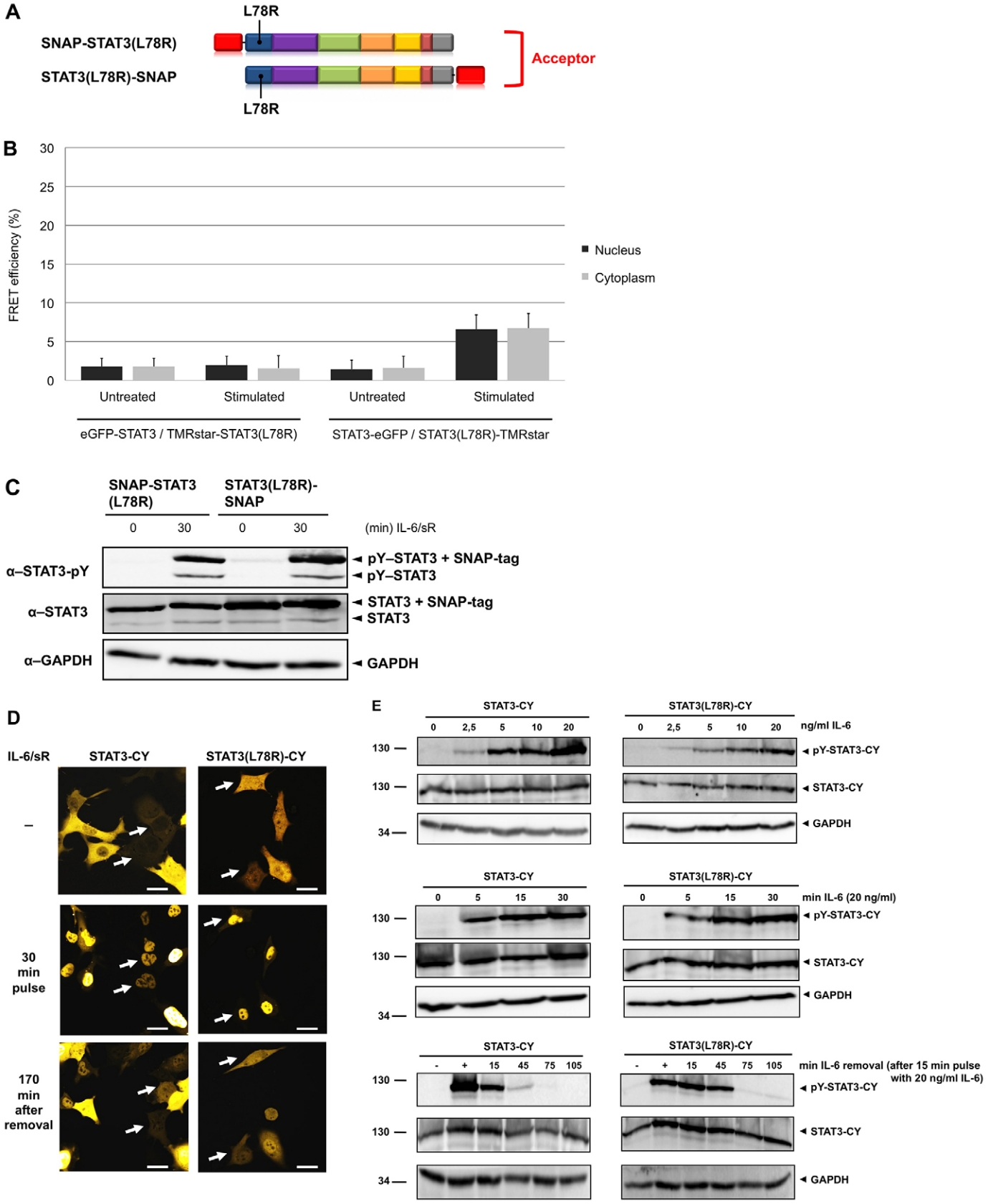

Fig. 5. See next page for legend.

Journal of Cell Science (2014) 127, 1899–1910 doi:10.1242/jcs.137422

Fig. 5. Characterization of the STAT3 L78R mutant. (A) Mutated STAT3 acceptor constructs for FRET imaging. The SNAP tag as a labelling site is located N- or C-terminally on the host molecule carrying the L78R amino acid mutation in the N-terminal region. (B) The L78R mutation prevents the dimerization of latent STAT3. HeLa cells were transfected with the indicated donor/acceptor pairs, labelled with TMRstar substrate, stimulated with IL-6 and soluble IL-6 receptor or left untreated, fixed and used for FRET imaging (mean±s.d., n=35 cells). (C) Phosphorylation of N-terminally mutated STAT3 constructs upon transient transfection. HeLa cells were transfected with the indicated expression vectors encoding SNAP–STAT3(L78R) or STAT3(L78R)–SNAP. Cells were stimulated with 20 ng/ml IL-6 and 500 ng/ml soluble IL-6 receptor (sR) for 30 minutes or left unstimulated. Lysates were analysed by western blotting using antibodies against STAT3 phosphotyrosine 705 (pY-STAT3) and STAT3. (D) Nuclear translocation of STAT3(L78R)-CY. MEF$^{\Delta/\Delta}$ cells stably transfected with fluorescent STAT3-CY wild-type or STAT3(L78R)-CY mutant were observed by confocal live-cell imaging. Cells were pulse-stimulated with 20 ng/ml IL-6 and 500 ng/ml soluble IL-6 receptor for 30 min. Cells were washed with PBS and supplied with fresh medium and observed for another 170 min. Because cells move during the course of the experiment, selected cells are marked with arrows. Scale bars: 20 µm. (E) Tyrosine phosphorylation of STAT3(L78R)-CY. MEF$^{\Delta/\Delta}$ cells stably transfected with fluorescent STAT3-CY wild-type or STAT3(L78R)-CY mutant were stimulated with 20 ng/ml IL-6 or the indicated concentrations for 20 min (upper panel), as indicated (middle panel) or pulse-stimulated for 15 min (+) and analysed after removal of IL-6 for the indicated times (lower panel). All stimulations were performed in the presence of 500 ng/ml soluble IL-6 receptor. Cellular lysates were prepared and analysed by western blotting using the antibodies as indicated.

after cytokine stimulation (nucleus, 11.39%±1.90; cytoplasm, 13.20%±2.78) showed a similar FRET efficiency to the eGFP–STAT3 and STAT3–TMRstar pair prior to or after activation (data not shown). In the experiments with double-labelled wild-type STAT3 we cannot exclude the intermolecular FRET signal from our detection system. However, the monomeric R609Q mutant showed high intramolecular FRET efficiency values (nucleus, 11.27%±2.16; cytoplasm, 10.95%±2.45) similar to that of the activated wild-type, indicating the same structural organization of this mutant monomer as the activated dimer (Fig. 6C).

These results suggest that mutation of the R609 residue in the SH2 domain not only prevents the interaction between phosphotyrosine motifs and the binding pocket in the SH2 domain, but leads to a complete reorientation of the SH2 domain (detected as high intramolecular FRET efficiency between the N- and C-terminal domains), disrupting the capability of the SH2 domain to additionally stabilize the preformed dimers. The R609Q mutant reflects a STAT3 form that structurally mimics the activated state, rendering the molecule unable to interact with activated and latent STAT3.

DISCUSSION

Our FRET experiments on latent STAT3 revealed closely associated NTDs that rearrange upon activation and DNA binding as indicated by the loss of nuclear FRET of the N-terminally labelled protomers upon stimulation of cells. Previous work from our laboratory (Vogt et al., 2011) showed that the deletion of the NTD abrogated the formation of latent STAT3 dimers. A similar function of the NTD in formation of latent dimers was shown for STAT5a (Neculai et al., 2005), STAT1 (Mao et al., 2005) and STAT4 (Vinkemeier et al., 1998). FRET experiments with the isolated N-terminal fragment of STAT3 support the idea of homotypic interactions of the NTDs instead of cross reactions with other domains of STAT3. These findings are

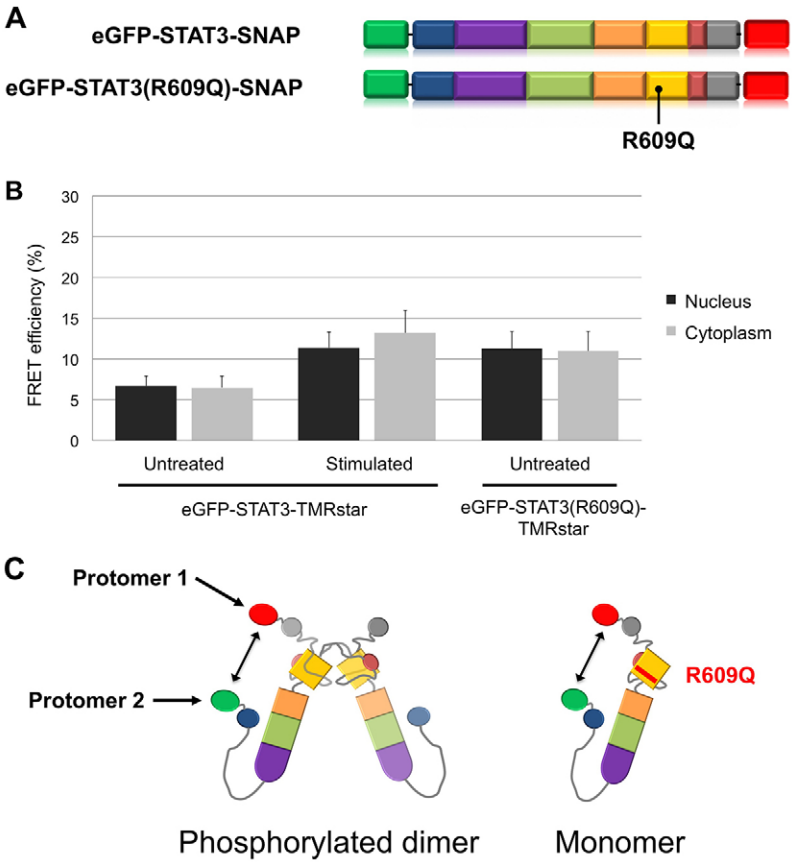

Fig. 6. Intramolecular FRET measurements on wild-type and STAT3 R609Q mutant. (A) STAT3 constructs used for intramolecular FRET measurements. To generate samples for intramolecular FRET analysis, the donor (eGFP, green) and acceptor (SNAP tag coupled with TMRstar substrate, red) were fused to the N- and C-terminus, respectively of the same host molecule. (B) Summary of intramolecular FRET measurements on wild-type and R609Q mutant STAT3. Similar to the intermolecular FRET results, an increased efficiency was detectable after cytokine addition, indicating a more sensitive detection of intermolecular FRET signal. The R609Q mutated monomer STAT3 form showed similar FRET efficiencies as the activated STAT3, indicating a similar orientation of the C- and N-terminal domains in the mutant monomer and in the activated dimer form (mean±s.d., n=30 cells). (C) Effect of R609 mutation on STAT3 structure. Mutation of the R609 residue drives the STAT3 monomer form to a similar structural organization as the activated dimer. This modification in the SH2 domain leads to the complete inability of STAT3 to form dimers prior to or after cytokine addition. Proposed localizations of the fluorophores in activated dimer and R609Q mutated monomeric STAT3 structures are highlighted in green (donor, eGFP) and red (acceptor, TMRstar).

Journal of Cell Science (2014) 127, 1899–1910 doi:10.1242/jcs.137422

in good agreement with previously published data based on other STAT family members (Ota et al., 2004; Wenta et al., 2008). Native gel electrophoresis showed that dimerization of nonphosphorylated STAT3 can be inhibited by the coexpression of the wild-type NTD (SNAP–NTD) demonstrating that the preformed dimers are to a large extent stabilized by homotypic NTD–NTD interactions.

Tetramerization of STAT3 has been shown to be essential for the maximal transcriptional activation of the α2-macroglobulin gene promoter (Zhang and Darnell, 2001). This cooperative binding of STAT dimers on specific DNA target sites is also mediated by homotypic interactions between NTDs (Vinkemeier et al., 1996; Xu et al., 1996). Upon overexpression of wild-type NTD, a significant downregulation of the α2-macroglobulin promoter was detectable compared to non-transfected or empty-vector-transfected samples, demonstrating the capability of SNAP-NTD construct to inhibit the tetramerization of STAT3. In agreement with our results, the same effect was achieved with the use of a STAT3-NTD-based inhibitor peptide (STAT3-Hel2A) on an acute-phase response element (APRE) luciferase reporter (Timofeeva et al., 2007).

Additionally, we focused on the crucial residue in the NTD, which is involved in mediating and stabilizing the homotypic interaction. Based on the somatic mutation found in inflammatory hepatocellular tumours (Pilati et al., 2011) targeting the NTD, we generated a construct encoding the N-terminal fragment with a L78R amino acid mutation. No interaction of the mutant NTD with full-length STAT3 protein was detectable, suggesting that the L78 residue is a promising target for further investigations. In support of our findings with the isolated NTDs, FRET measurements on L78R mutated STAT3 showed no detectable dimers prior to activation. These results suggest a similar NTD–NTD interface in STAT3 as was previously proposed for STAT4 and STAT1 (Chen et al., 2003), where the hydrophobic residues L77 and L78 are involved in the homodimerization of these domains. Mutations of these residues to alanine did however not completely prevent latent dimer formation of STAT3 (Vogt et al., 2011). Thus, a stronger disturbance of the dimer interface, such as the replacement of the hydrophic leucine residue by a charged arginine residue, is required to achieve a monomeric population of latent STAT3.

In the context of IHCA, STAT3(L78R) has been reported to be a weakly constitutively active mutant. In our hands, upon transient overexpression in HeLa cells in the presence of endogenous STAT3 wild-type as well as upon stable expression in $MEF^{\Delta/\Delta}$ cells lacking endogenous STAT3, hardly any constitutive phosphorylation was detectable. However, under steady-state conditions, a greater portion of the L78R mutant is located in the nucleus compared to wild-type, as has been observed for STAT3 lacking the NTD (Vogt et al., 2011). Sensitivity to IL-6 stimulation is similar for STAT3 wild-type and the L78R mutant. In this respect, STAT3 resembles STAT1 and is different from STAT4, which requires latent dimer formation for activation (Ota et al., 2004). However, upon pulse-stimulation, phosphorylation of STAT3(L78R) is slightly prolonged. This does not translate into a prolonged nuclear localization, most probably because of the different time windows of dephosphorylation (minutes) and redistribution (hours). Interestingly the NTD of STAT3 has been shown to be important for the recruitment of coactivators such as most recently described for FoxP3 (Hossain et al., 2013). It would be interesting to know whether this kind of interaction is also mediated through the L78 interface and whether the disturbance of such interactions through the L78R mutation contributes to IHCA.

The NTD of STAT3 forms dimers through a low affinity interaction (K_d=3.7 mM) compared to the NTDs of STAT1 and STAT4 (K_d=23.3 μM and 2.7 μM, respectively) (Wenta et al., 2008) suggesting that other structural regions are involved in dimer stabilization of full-length STAT3. The crystal structure of the unphosphorylated STAT3 core fragment (lacking the NTD and transactivation domain) revealed no evidence of other structural domains being involved in preformed dimer formation, such as the coiled-coil domain or DNA-binding domain (Ren et al., 2008), in contrast to STAT1 and STAT5 (Mao et al., 2005; Neculai et al., 2005). In particular, the interface involving the F172 residue in the anti-parallel STAT1 dimer is not conserved in STAT3 (Ren et al., 2008). Our measurements on C-terminally truncated STAT3 showed that deletion of the transactivation domain does not affect latent dimer formation (data not shown). However, FRET measurements on SH2-mutated STAT3(R609Q) revealed the need for an intact SH2 domain for the formation of latent dimers and suggested that there are SH2 homotypic interactions prior to activation (Kretzschmar et al., 2004). Our intramolecular FRET measurements on STAT3R609Q (Fig. 6B) indicate that this mutation not only affects interaction with phosphotyrosine motifs but disturbs the overall structure of the SH2 domain resulting in a monomer, which mimics the structural organization of the activated STAT3 dimer. This modification possibly interferes with regions in the SH2 domain that are involved in dimerization of latent STAT3 by generating an additional stabilizing interface

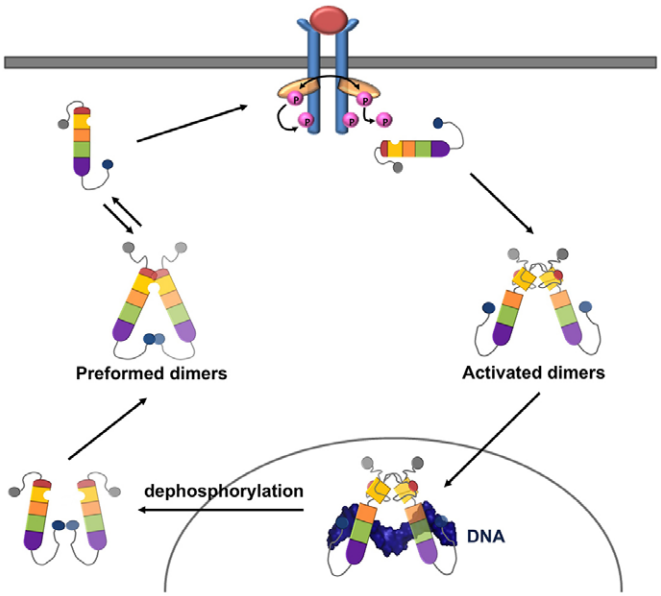

Fig. 7. Preformed and activated STAT3 dimers in the JAK-STAT3 pathway. Monomers are associated in the latent state (unphosphorylated dimers) in a parallel orientation. This dimer is mostly stabilized by homotypic interactions between the N-terminal domains, and orientates the protomers in a form, which structurally allows the separate SH2 domains to interact with each other resulting in additional stabilization. The phosphorylated monomers are associated in the activated dimer form (stabilized by phosphotyrosine–SH2 interactions), which translocates to the nuclear compartment where they bind to specific DNA sequences. After inactivation (dephosphorylation) STAT3 is transported to the cytoplasmic region, and through an intermediate state, forms latent dimers in equilibrium with monomers.

between the SH2 fragments. Previously published data have demonstrated that the isolated STAT3 SH2 domain interacts with itself, and these dimerized SH2 domains are unable to interact with phosphopeptides (Haan et al., 1999). Interestingly, in HIES, heterozygous mutations (missense or single-codon in-frame microdeletions) in the DNA-binding and SH2 domains of STAT3 (Holland et al., 2007) result in the expression of full length but dysfunctional STAT3 molecules. The mutations targeting the DNA-binding domain have been shown to have dominant-negative effects on the wild-type form (Minegishi et al., 2007), whereas the amino acid changes in the SH2 domain (S611N and F621V), similar to R609Q mutation, abrogate the dimerization of STAT3 upon activation (He et al., 2012).

Our findings identify the SH2 domain as a secondary stabilizer of latent STAT3 dimers leading to a parallel orientation of the protomers similar to that of activated STAT3 (Fig. 7). This is in contrast to the antiparallel dimers of latent STAT1 and STAT5 where the SH2 domains are localized at the opposite ends of the dimer (Mao et al., 2005; Mertens et al., 2006; Neculai et al., 2005). This parallel association could explain why, under some circumstances, latent STAT3 is capable of DNA binding (Nkansah et al., 2013; Timofeeva et al., 2012) and gene induction (Yang et al., 2005).

MATERIALS AND METHODS

Plasmid constructs

Differently labelled STAT3 constructs for FRET analysis were generated with the use of pcDNA5/FRT/TO expression vector (Invitrogen, USA). pcDNA5/FRT/TO-STAT3-YFP (Herrmann et al., 2007) was used as a template for cloning the constructs. The labelling tags eGFP and SNAP were derived from peGFP-N1 vector (Clontech, USA) and pcDNA5/FRT/TO-SNAP-YFP (Recker et al., 2011), respectively, and amplified by PCR with the appropriate primers to insert the restriction sites for the cloning procedure. R609Q mutated STAT3 was created from pSVL-STAT3(R609Q)-YFP, described previously (Herrmann et al., 2004). Site directed mutagenesis was performed with the QuikChange II XL Kit (Agilent Technologies, USA) to introduce the L78R mutation (underlined codon) into STAT3 using the following primer pair: 5′-CAAGAGTCCA-ATGTCCGCTA TCAGCACAACCTTC-3′ and 5′-GAAGGTTGTGC-TGATAGCGGACATTGGACTCTTG-3′.

Cytokines and cytokine receptors

Recombinant human IL-6 (1400 U/µl) and soluble IL-6 receptor were prepared as described previously (Arcone et al., 1991; Weiergräber et al., 1995).

Cell culture and tranfection

Human cervix adenocarcinoma (HeLa) cells were cultivated in Phenol Red free DMEM-medium (Gibco, Germany), supplemented with 10% FCS and 1% penicillin/streptomycin. Human liver hepatocellular carcinoma (HepG2) cells were cultivated in DMEM/F12-Medium (Gibco, Germany), supplemented with 10% FCS and 1% penicillin/streptomycin. The cells were incubated at 37℃ in a humidified atmosphere containing 5% CO_2. Transfection was performed transiently, when cells reached a density of 60–80% confluence, by using the transfection reagent TransIT-LT1 (Mirus Bio LLC, USA), and OPTIMEM (Gibco, Germany) as serum-free medium. Conditions and protocols were used according to the manufacturer's instructions. $MEF^{\Delta/\Delta}$ cells stably transfected with STAT3(L78R)-CY have been generated as described earlier for STAT3-CY wild-type (Vogt et al., 2011) using the Flip-In T-REx system (Invitrogen, USA) that guarantees integration of the different transgenes at identical genomic sites.

Immunoblot analysis

HeLa cells were cultured on six-well plates. The cells were stimulated with 20 ng/ml IL-6 and 500 ng/ml soluble IL-6 receptor for 30 minutes or left untreated and lysed as described previously (Vogt et al., 2011). The lysates were analysed by SDS-PAGE, western blotting and immunodetection using antibodies directed against phosphotyrosine 705 of STAT3 (Cell Signaling Technology, Danvers, MA) and STAT3 (H190; Santa Cruz Biotechnology, Santa Cruz, CA).

SNAP tag labelling procedure

The labelling of the SNAP tag fusion proteins was performed using SNAP-Cell TMRstar substrate, a cell-permeable fluorescent label based on Tetramethylrhodamine (New England Biolabs, USA). The labelling procedure was carried out according to the manufacturer's protocol.

Confocal microscopy and live-cell imaging

HeLa cells were examined with a LSM 710 confocal microscope (Carl Zeiss, Germany) using a 40×, 1.1 NA water immersion objective. For fixation, cells were seeded and grown on LabTek four-well chamber slides (Nunc, Thermo Fisher Scientific, USA) in Phenol-Red-free medium. After removing the medium, cells were washed two times in phosphate-buffered saline (PBS) containing 1 mM $MgCl_2$ and 0.1 mM $CaCl_2$ (PBS^{++}). Fixation was performed by addition of 200 µl methanol to the cells, followed by incubation in the dark, for 20 minutes at room temperature. After incubation, the cells were washed once with PBS^{++} and quenched with 50 mM NH_4Cl (diluted in PBS^{++}) for 5 minutes. Coverslips were mounted with Immu-Mount (Thermo Fisher Scientific, USA) and the samples were kept in the dark until further investigation. For live-cell imaging, cells were plated on 35-mm glass-bottomed dishes (Ibidi, Germany) in Phenol-Red-free medium 48 hours before the experiment and transfected as described above. Cells were imaged at 37℃ and 5% CO_2 in the cell incubator of a Zeiss LSM 710 microscope (Carl Zeiss, Germany).

FRET measurements

In this work we applied the acceptor photobleaching (APB) method. In APB, the acceptor fluorophore is selectively bleached with a strong laser pulse in a defined area (region of interest). The fluorescence intensity of the donor fluorophore is analysed before (D_{pre}) and after the bleaching procedure (D_{post}). The difference between these donor intensities enables the calculation of the FRET efficiency ($FRET_{eff}$) (Wouters et al., 1998) using the following equation:

$$FRET_{eff} = (D_{post} - D_{pre}) / D_{post}.$$

For FRET measurements, HeLa cells were examined with a LSM 710 confocal microscope (Carl Zeiss, Germany) using a 40×, 1.1 NA water immersion objective with 3× zoom, and 512×512 pixel resolution. Emission filters were 505–550 nm for 488 nm excitation (eGFP detection, donor channel), and 575–616 nm for 561 nm excitation (TMRstar detection, acceptor channel). Images were collected using multi-track mode, with 2% laser intensity. Two eGFP and TMRstar image pairs were collected before the photobleaching. Bleaching was performed in a rectangular region of interest (ROI) in TMRstar channel using the 561-nm laser line at maximum laser power (100% transmission) for 100 iterations. Cells displaying comparable levels of eGFP and TMRstar were selected for FRET analysis to avoid artefacts and interferences from different donor-to-acceptor ratios. The measurement setup was established and optimized from the experiments based on the positive control (SNAP tag fused to eGFP and labelled with TMR-star substrate, TMRstar–eGFP). FRET efficiencies (%) were calculated using Zen software (Carl Zeiss, Germany), based on the equation described above, taking into account the threshold and background noise in each channel. For live-cell FRET imaging, HeLa cells were plated and seeded on eight-well µ-Slides (Ibidi, Germany), which were placed, 24 hours after transfection, in the cell incubator of a Zeiss LSM 710 microscope (Carl Zeiss, Germany) at 37℃ under 5% CO_2. FRET measurements were performed using the same setup (gain settings, resolution, optical components) as described above.

Blue-native PAGE

HeLa cells were transfected with STAT3–YFP and increasing amounts of the SNAP–NTD-encoding expression vector. Cells were left unstimulated and lysed with the NativePAGE™ Sample Prep Kit (Invitrogen, UK) with 1% (final volume) DDM (n-dodecyl-β-maltoside) as detergent. The lysates were mixed with Coomassie Brilliant Blue G-250 and separated on a 4–16% gradient gel using the NativePAGE™ Novex Bis-Tris gel system (Invitrogen, UK), and the protein complexes were separated overnight at 4°C. Following electrophoresis, the gel was analysed with a fluorescence scanner to visualize the STAT3–YFP signal by using a fluorescence scanner (Typhoon, GE Healthcare, UK). The probe was excited with 488-nm laser line and the emission detected using 515–555 nm band filter setting.

Reporter gene assay

HepG2 cells were grown in six-well plates and transfection was performed with 1 µg β-galactosidase expression vector (pCR3lacZ, Pharmacia, Sweden), 300 ng of luciferase reporter construct (α2-macroglobulin) and the indicated plasmid constructs using the TransIT-LT1 transfection reagent (Mirus Bio LLC, USA) according to the manufacturer's instructions. After 24 hours, cells were stimulated for 4 hours, harvested, and luciferase and β-galactosidase activity were measured in triplicates. Luciferase assays were performed using a luciferase assay kit (Promega, Germany) and values were normalized to transfection efficiencies derived from β-Gal expression.

Competing interests

The authors declare no competing interests.

Author contributions

T.D. designed and performed most of the experiments, interpreted the data and wrote a first draft of the manuscript. A.M. characterized the STAT3(L78R) mutant. D.F. contributed to confocal microscopy and critical discussion of the data. H.S.-V. and A.K. generated most of the plasmid constructs and provided technical assistance on multiple levels. G.M.-N. initiated the study, interpreted the data and critically revised the manuscript. All authors have read and approved the final manuscript.

Funding

The project was funded by grants from the Deutsche Forschungsgemeinschaft (SFB 542); and the European Community (Marie Curie Research and Training Network ReceptEUR). This work was also supported by the 'Immunohistochemisty and Confocal Microscopy Facility', a core facility of the Interdisciplinary Center for Clinical Research (IZKF) Aachen within the Faculty of Medicine at RWTH Aachen University. A.M. is supported through a scholarship of the Studienstiftung des Deutschen Volkes.

References

Aggarwal, B. B., Kunnumakkara, A. B., Harikumar, K. B., Gupta, S. R., Tharakan, S. T., Koca, C., Dey, S. and Sung, B. (2009). Signal transducer and activator of transcription-3, inflammation, and cancer: how intimate is the relationship? *Ann. N. Y. Acad. Sci.* **1171**, 59-76.

Arcone, R., Pucci, P., Zappacosta, F., Fontaine, V., Malorni, A., Marino, G. and Ciliberto, G. (1991). Single-step purification and structural characterization of human interleukin-6 produced in Escherichia coli from a T7 RNA polymerase expression vector. *Eur. J. Biochem.* **198**, 541-547.

Becker, S., Groner, B. and Müller, C. W. (1998). Three-dimensional structure of the Stat3beta homodimer bound to DNA. *Nature* **394**, 145-151.

Berney, C. and Danuser, G. (2003). FRET or no FRET: a quantitative comparison. *Biophys. J.* **84**, 3992-4010.

Braunstein, J., Brutsaert, S., Olson, R. and Schindler, C. (2003). STATs dimerize in the absence of phosphorylation. *J. Biol. Chem.* **278**, 34133-34140.

Chen, X., Bhandari, R., Vinkemeier, U., Van Den Akker, F., Darnell, J. E., Jr and Kuriyan, J. (2003). A reinterpretation of the dimerization interface of the N-terminal domains of STATs. *Protein Sci.* **12**, 361-365.

Cimica, V., Chen, H. C., Iyer, J. K. and Reich, N. C. (2011). Dynamics of the STAT3 transcription factor: nuclear import dependent on Ran and importin-β1. *PLoS ONE* **6**, e20188.

Droescher, M., Begitt, A., Marg, A., Zacharias, M. and Vinkemeier, U. (2011). Cytokine-induced paracrystals prolong the activity of signal transducers and activators of transcription (STAT) and provide a model for the regulation of protein solubility by small ubiquitin-like modifier (SUMO). *J. Biol. Chem.* **286**, 18731-18746.

Haan, S., Hemmann, U., Hassiepen, U., Schaper, F., Schneider-Mergener, J., Wollmer, A., Heinrich, P. C. and Grötzinger, J. (1999). Characterization and binding specificity of the monomeric STAT3-SH2 domain. *J. Biol. Chem.* **274**, 1342-1348.

Haan, S., Kortylewski, M., Behrmann, I., Müller-Esterl, W., Heinrich, P. C. and Schaper, F. (2000). Cytoplasmic STAT proteins associate prior to activation. *Biochem. J.* **345**, 417-421.

He, J., Shi, J., Xu, X., Zhang, W., Wang, Y., Chen, X., Du, Y., Zhu, N., Zhang, J., Wang, Q. et al. (2012). STAT3 mutations correlated with hyper-IgE syndrome lead to blockage of IL-6/STAT3 signalling pathway. *J. Biosci.* **37**, 243-257.

Hemmann, U., Gerhartz, C., Heesel, B., Sasse, J., Kurapkat, G., Grötzinger, J., Wollmer, A., Zhong, Z., Darnell, J. E. J., Jr, Graeve, L. et al. (1996). Differential activation of acute phase response factor/Stat3 and Stat1 via the cytoplasmic domain of the interleukin 6 signal transducer gp130. II. Src homology SH2 domains define the specificity of stat factor activation. *J. Biol. Chem.* **271**, 12999-13007.

Herrmann, A., Sommer, U., Pranada, A. L., Giese, B., Küster, A., Haan, S., Becker, W., Heinrich, P. C. and Müller-Newen, G. (2004). STAT3 is enriched in nuclear bodies. *J. Cell Sci.* **117**, 339-349.

Herrmann, A., Vogt, M., Mönnigmann, M., Clahsen, T., Sommer, U., Haan, S., Poli, V., Heinrich, P. C. and Müller-Newen, G. (2007). Nucleocytoplasmic shuttling of persistently activated STAT3. *J. Cell Sci.* **120**, 3249-3261.

Holland, S. M., DeLeo, F. R., Elloumi, H. Z., Hsu, A. P., Uzel, G., Brodsky, N., Freeman, A. F., Demidowich, A., Davis, J., Turner, M. L. et al. (2007). STAT3 mutations in the hyper-IgE syndrome. *N. Engl. J. Med.* **357**, 1608-1619.

Hossain, D. M., Panda, A. K., Manna, A., Mohanty, S., Bhattacharjee, P., Bhattacharyya, S., Saha, T., Chakraborty, S., Kar, R. K., Das, T. et al. (2013). FoxP3 acts as a cotranscription factor with STAT3 in tumor-induced regulatory T cells. *Immunity* **39**, 1057-1069.

Huang, Y., Qiu, J., Dong, S., Redell, M. S., Poli, V., Mancini, M. A. and Tweardy, D. J. (2007). Stat3 isoforms, alpha and beta, demonstrate distinct intracellular dynamics with prolonged nuclear retention of Stat3beta mapping to its unique C-terminal end. *J. Biol. Chem.* **282**, 34958-34967.

Koskela, H. L., Eldfors, S., Ellonen, P., van Adrichem, A. J., Kuusanmäki, H., Andersson, E. I., Lagström, S., Clemente, M. J., Olson, T., Jalkanen, S. E. et al. (2012). Somatic STAT3 mutations in large granular lymphocytic leukemia. *N. Engl. J. Med.* **366**, 1905-1913.

Kretzschmar, A. K., Dinger, M. C., Henze, C., Brocke-Heidrich, K. and Horn, F. (2004). Analysis of Stat3 dimerization by fluorescence resonance energy transfer in living cells. *Biochem. J.* **377**, 289-297.

Levy, D. E. and Darnell, J. E., Jr (2002). Stats: transcriptional control and biological impact. *Nat. Rev. Mol. Cell Biol.* **3**, 651-662.

Mao, X., Ren, Z., Parker, G. N., Sondermann, H., Pastorello, M. A., Wang, W., McMurray, J. S., Demeler, B., Darnell, J. E., Jr and Chen, X. (2005). Structural bases of unphosphorylated STAT1 association and receptor binding. *Mol. Cell* **17**, 761-771.

Mertens, C., Zhong, M., Krishnaraj, R., Zou, W., Chen, X. and Darnell, J. E., Jr (2006). Dephosphorylation of phosphotyrosine on STAT1 dimers requires extensive spatial reorientation of the monomers facilitated by the N-terminal domain. *Genes Dev.* **20**, 3372-3381.

Minegishi, Y., Saito, M., Tsuchiya, S., Tsuge, I., Takada, H., Hara, T., Kawamura, N., Ariga, T., Pasic, S., Stojkovic, O. et al. (2007). Dominant-negative mutations in the DNA-binding domain of STAT3 cause hyper-IgE syndrome. *Nature* **448**, 1058-1062.

Mohr, A., Chatain, N., Domoszlai, T., Rinis, N., Sommerauer, M., Vogt, M. and Müller-Newen, G. (2012). Dynamics and non-canonical aspects of JAK/STAT signalling. *Eur. J. Cell Biol.* **91**, 524-532.

Ndubuisi, M. I., Guo, G. G., Fried, V. A., Etlinger, J. D. and Sehgal, P. B. (1999). Cellular physiology of STAT3: Where's the cytoplasmic monomer? *J. Biol. Chem.* **274**, 25499-25509.

Neculai, D., Neculai, A. M., Verrier, S., Straub, K., Klumpp, K., Pfitzner, E. and Becker, S. (2005). Structure of the unphosphorylated STAT5a dimer. *J. Biol. Chem.* **280**, 40782-40787.

Nkansah, E., Shah, R., Collie, G. W., Parkinson, G. N., Palmer, J., Rahman, K. M., Bui, T. T., Drake, A. F., Husby, J., Neidle, S. et al. (2013). Observation of unphosphorylated STAT3 core protein binding to target dsDNA by PEMSA and X-ray crystallography. *FEBS Lett.* **587**, 833-839.

O'Sullivan, L. A., Liongue, C., Lewis, R. S., Stephenson, S. E. and Ward, A. C. (2007). Cytokine receptor signaling through the Jak-Stat-Socs pathway in disease. *Mol. Immunol.* **44**, 2497-2506.

Ota, N., Brett, T. J., Murphy, T. L., Fremont, D. H. and Murphy, K. M. (2004). N-domain-dependent nonphosphorylated STAT4 dimers required for cytokine-driven activation. *Nat. Immunol.* **5**, 208-215.

Pilati, C., Amessou, M., Bihl, M. P., Balabaud, C., Nhieu, J. T., Paradis, V., Nault, J. C., Izard, T., Bioulac-Sage, P., Couchy, G. et al. (2011). Somatic mutations activating STAT3 in human inflammatory hepatocellular adenomas. *J. Exp. Med.* **208**, 1359-1366.

Recker, T., Haamann, D., Schmitt, A., Küster, A., Klee, D., Barth, S. and Müller-Newen, G. (2011). Directed covalent immobilization of fluorescently labeled cytokines. *Bioconjug. Chem.* **22**, 1210-1220.

Ren, Z., Mao, X., Mertens, C., Krishnaraj, R., Qin, J., Mandal, P. K., Romanowski, M. J., McMurray, J. S. and Chen, X. (2008). Crystal structure of unphosphorylated STAT3 core fragment. *Biochem. Biophys. Res. Commun.* **374**, 1-5.

Schröder, M., Kroeger, K. M., Volk, H. D., Eidne, K. A. and Grütz, G. (2004). Preassociation of nonactivated STAT3 molecules demonstrated in living cells

using bioluminescence resonance energy transfer: a new model of STAT activation? *J. Leukoc. Biol.* **75**, 792-797.
Stancato, L. F., David, M., Carter-Su, C., Larner, A. C. and Pratt, W. B. (1996). Preassociation of STAT1 with STAT2 and STAT3 in separate signalling complexes prior to cytokine stimulation. *J. Biol. Chem.* **271**, 4134-4137.
Stark, G. R. and Darnell, J. E., Jr (2012). The JAK-STAT pathway at twenty. *Immunity* **36**, 503-514.
Timofeeva, O. A., Gaponenko, V., Lockett, S. J., Tarasov, S. G., Jiang, S., Michejda, C. J., Perantoni, A. O. and Tarasova, N. I. (2007). Rationally designed inhibitors identify STAT3 N-domain as a promising anticancer drug target. *ACS Chem. Biol.* **2**, 799-809.
Timofeeva, O. A., Chasovskikh, S., Lonskaya, I., Tarasova, N. I., Khavrutskii, L., Tarasov, S. G., Zhang, X., Korostyshevskiy, V. R., Cheema, A., Zhang, L. et al. (2012). Mechanisms of unphosphorylated STAT3 transcription factor binding to DNA. *J. Biol. Chem.* **287**, 14192-14200.
Timofeeva, O. A., Tarasova, N. I., Zhang, X., Chasovskikh, S., Cheema, A. K., Wang, H., Brown, M. L. and Dritschilo, A. (2013). STAT3 suppresses transcription of proapoptotic genes in cancer cells with the involvement of its N-terminal domain. *Proc. Natl. Acad. Sci. USA* **110**, 1267-1272.
Vinkemeier, U., Cohen, S. L., Moarefi, I., Chait, B. T., Kuriyan, J. and Darnell, J. E., Jr (1996). DNA binding of in vitro activated Stat1 alpha, Stat1 beta and truncated Stat1: interaction between NH2-terminal domains stabilizes binding of two dimers to tandem DNA sites. *EMBO J.* **15**, 5616-5626.
Vinkemeier, U., Moarefi, I., Darnell, J. E., Jr and Kuriyan, J. (1998). Structure of the amino-terminal protein interaction domain of STAT-4. *Science* **279**, 1048-1052.
Vogt, M., Domoszlai, T., Kleshchanok, D., Lehmann, S., Schmitt, A., Poli, V., Richtering, W. and Müller-Newen, G. (2011). The role of the N-terminal domain in dimerization and nucleocytoplasmic shuttling of latent STAT3. *J. Cell Sci.* **124**, 900-909.
Weiergräber, O., Hemmann, U., Küster, A., Müller-Newen, G., Schneider, J., Rose-John, S., Kurschat, P., Brakenhoff, J. P., Hart, M. H., Stabel, S. et al. (1995). Soluble human interleukin-6 receptor. Expression in insect cells, purification and characterization. *Eur. J. Biochem.* **234**, 661-669.
Wenta, N., Strauss, H., Meyer, S. and Vinkemeier, U. (2008). Tyrosine phosphorylation regulates the partitioning of STAT1 between different dimer conformations. *Proc. Natl. Acad. Sci. USA* **105**, 9238-9243.
Wouters, F. S., Bastiaens, P. I., Wirtz, K. W. and Jovin, T. M. (1998). FRET microscopy demonstrates molecular association of non-specific lipid transfer protein (nsL-TP) with fatty acid oxidation enzymes in peroxisomes. *EMBO J.* **17**, 7179-7189.
Xu, X., Sun, Y. L. and Hoey, T. (1996). Cooperative DNA binding and sequence-selective recognition conferred by the STAT amino-terminal domain. *Science* **273**, 794-797.
Yang, J., Chatterjee-Kishore, M., Staugaitis, S. M., Nguyen, H., Schlessinger, K., Levy, D. E. and Stark, G. R. (2005). Novel roles of unphosphorylated STAT3 in oncogenesis and transcriptional regulation. *Cancer Res.* **65**, 939-947.
Yu, H. and Jove, R. (2004). The STATs of cancer – new molecular targets come of age. *Nat. Rev. Cancer* **4**, 97-105.
Zhang, X. and Darnell, J. E., Jr (2001). Functional importance of Stat3 tetramerization in activation of the alpha 2-macroglobulin gene. *J. Biol. Chem.* **276**, 33576-33581.
Zhang, T., Seow, K. T., Ong, C. T. and Cao, X. (2002). Interdomain interaction of Stat3 regulates its Src homology 2 domain-mediated receptor binding activity. *J. Biol. Chem.* **277**, 17556-17563.